

Prediction of cross-fitness for adaptive evolution to different environmental conditions: Consequence of phenotypic dimensional reduction

Takuya U. Sato^{1,2,*}, Chikara Furusawa^{1,2,†} and Kunihiko Kaneko^{3,4,‡}

¹Center for Biosystems Dynamics Research (BDR), RIKEN, 6-2-3 Furuedai, Suita, Osaka 565-0874, Japan

²Universal Biology Institute, Graduate School of Science, The University of Tokyo, Faculty of Science Bldg. 1, 7-3-1 Hongo, Bunkyo-ku, Tokyo 113-0033, Japan

³Center for Complex Systems Biology, Universal Biology Institute, University of Tokyo, Komaba, Tokyo 153-8902, Japan

⁴The Niels Bohr Institute, University of Copenhagen, Blegdamsvej 17, Copenhagen, 2100, Denmark

 (Received 16 September 2022; revised 22 February 2023; accepted 17 October 2023; published 11 December 2023)

How adaptive evolution to one environmental stress improves or suppresses adaptation to another is an important problem in evolutionary biology. For instance, in microbiology, the change of resistance to one antibiotic by resistance acquisition by another drug is a critical issue that has been investigated as cross-resistance. Recent experiments on bacteria have suggested that the cross-resistance of their evolution to various stressful environments can be predicted based on the transcriptome changes after evolution under the corresponding stresses. However, there are no studies so far that explain a possible theoretical relationship between cross-resistance and changes in the transcriptome, which causes high-dimensional changes to cell phenotype. In the present paper, we show that a correlation exists between fitness change in stress tolerance evolution and response to the environment, using a cellular model with a high-dimensional phenotype and establishing the relationship theoretically by formulating a macroscopic potential theory against environmental and genetic changes. Finally, we applied the theory to experimental data on bacterial evolution under antibiotics, which demonstrates the theoretically predicted correlation between the fitness changes by evolution and transcriptome changes upon environmental stresses. Thus, evolution is predicted from transcriptome information in response to stresses before evolution.

DOI: [10.1103/PhysRevResearch.5.043222](https://doi.org/10.1103/PhysRevResearch.5.043222)

I. INTRODUCTION

Generally, organisms change their state to adapt to various environmental stresses. This ability is thought to have been acquired through evolution [1,2]. Those that evolved to adapt to one environment may increase or decrease the degree of their adaptation to another environment. For example, adaptive evolution to one stressful environment may increase or decrease fitness to manage another stress as compared with that of the organism before evolution. This correlated change in fitness is called cross-resistance [3–11]. If the adaptive evolution to one environmental stress increases or decreases the fitness for another, the cross-resistance is positive or negative, respectively. In medicine, understanding the cross-resistance of bacteria to different antibiotics is a crucial issue.

Can such cross-resistance be predicted? Extensive studies have been conducted to uncover specific genetic mutations which allow adaptive evolution to individual environmental stresses and to unveil functional changes that occur as a result of such mutations. Molecular changes caused by

mutations have been identified in certain genes which allow for resistance to environmental stress [12,13]. However, the detailed mechanisms of cross-resistance remain unclear. Cross-resistance between different environmental conditions involves interactions among diverse components that are influenced by the mutation and are not explained directly by specific molecular changes. Examination of the correlation between fitness changes across different environmental conditions using standard molecular biology methods that focus on a one-to-one correspondence between genes and functions is not easy.

How can we compare adaptive evolution under different environmental conditions? For this purpose, we need to consider changes to the cellular state that is shaped by a wide variety of components. Such a cellular state can be represented by the concentrations of these components. Changes in the cellular state in response to environmental changes, such as antibiotics, temperature, and nutritional conditions, will lead to a change in the growth of a cell. The correlation of changes in the cellular state across different environmental changes will provide information on how organisms evolve to them. Such information involves high-dimensional data that characterize the cellular state.

Recent advances in experimental techniques have enabled the acquisition of high-dimensional data of cellular states, such as the transcriptome, proteome, and metabolome [14–16]. Using these high-dimensional data, a detailed analysis of the cellular state is now possible. However, how can we extract relevant information from

*takuya.sato.zs@riken.jp

†chikara.furusawa@riken.jp

‡lapikaneko@gmail.com

high-dimensional data with thousands of components to obtain the correlation between evolutionary adaptation to different conditions?

A recent experimental report examined transcriptome changes throughout the evolution of bacteria in response to a variety of environmental stresses [8,17]. In these studies, the authors measured the cross-resistance, that is, how adaptive evolution to one environment, $E^{(1)}$, changed the growth rate of bacteria in another environment, $E^{(2)}$. Then, by measuring transcriptome changes through adaptive evolution, they constructed a low-dimensional linear model for these changes, explaining the observed cross-resistance. Notably, the environmental stresses adopted in their experiments had a variety of molecular effects on cells. The transcriptome of *E. coli* used in their experiment was high-dimensional data with over 4000 dimensions. Despite this complexity, low-dimensional information extracted from high-dimensional information is suggested to be relevant to predict cross-resistance to a variety of conditions to a certain degree.

If cellular states moved throughout the entire high-dimensional space during adaptive evolution to various stress environments, changes in phenotype (i.e., cellular state) in response to different stress environments would not be correlated, and predictions of cross-resistance by the environmental response would not be possible. However, such predictions may be possible if transcriptome changes due to adaptive evolution are restricted to a relatively low-dimensional subspace. Is there general support for a such low-dimensional reduction in adaptive changes to cellular states?

Several recent experiments have suggested that changes in cellular state in response to environmental stresses are constrained in low-dimensional space [18–23]. Changes in the transcriptome of *E. coli* across various stress environments were found to be strongly correlated. Horinouchi *et al.* also showed that transcriptomic changes in independent evolutionary lineages converge along the common principal component (PC) space in the adaptive evolution of *E. coli* under ethanol stress. These results suggest that phenotypic changes in the adaptation and evolution of cells in response to environmental stress occur within a low-dimensional space.

How are phenotypic changes constrained to a low-dimensional space? By simulating a catalytic chemical reaction network model with thousands of components, it was found that high-dimensional concentration changes in response to environmental or mutational changes are constrained to a common low-dimensional space as a result of evolution to increase the fitness [24–26]. This constraint is then formulated in terms of dynamical systems theory as a separation of a few slow eigenmodes for the relaxation dynamics of the rate equation representing the cellular state changes.

Can we, then, theoretically predict cross-resistance using the information in such low-dimensional constraints [27]? In the presence of phenotypic constraints, responses to environmental and evolutionary changes are restricted to a common, lower-dimensional subspace. Accordingly, one does not need the entire high-dimensional data to predict the fitness change; information within the low-dimensional subspace will be sufficient to estimate the fitness changes across environmental conditions. Thus, the information needed to predict

cross-resistance is significantly reduced. In the present study, we first used a gene regulatory network (GRN) model to demonstrate such low-dimensional phenotypic constraints by evolution, and then demonstrated that cross-resistance is predicted by cellular responses to stress before evolution by taking advantage of phenotypic constraints [28–33]. Then, to show that the result is universal, independent of the specific choice of GRN model, we formulate a macroscopic potential theory, where the fitness is represented as a function of environmental and genetic changes, from which the cross-resistance is predicted generally in terms of the response to antibiotics in before evolution. This allows for experimental verification of the theoretical predictivity as will be presented.

The remainder of this paper is organized as follows: In Sec. II we introduce the GRN model of a cell used in the present study and describe the procedure of simulated evolution. Next, in Sec. III we show that phenotypic constraints are produced when the GRNs are evolved under fitness to satisfy multiple input-output relationships. We demonstrate that the degree of the phenotypic constraint acquired through evolution is determined by the number and strength of the postulated input-output relationships. We also explain such constraints in terms of the nature of gene regulatory matrices. In Sec. IV we show the results of simulations of adaptive evolution to a variety of environmental stresses, by using the evolved GRNs obtained in Sec. III as the ancestor. Then we computed the cross-fitness, that is, the fitness of a cell that has evolved under another environment for a new environment. We demonstrated that this cross-fitness is approximated using low-dimensional variables along with phenotypic constraint coordinates. In particular, when a P -dimensional phenotypic constraint exists, the cross-fitness and cross-resistance that are desired from it are approximately described by a function of P variables. Then the cross-fitness as a result of evolution is predicted by the correlation in transcriptome changes upon environmental stresses. In Sec. V the approximate form of cross-fitness in Sec. IV is derived by assuming that fitness is given by a potential function of low-dimensional environmental and genetic coordinates. In Sec. VI we apply the present theory to experimental data of evolution of resistance to antibiotics in *E. coli*. The experimental data well reproduce the predicted correlation between the cross-fitness and transcriptome changes. In Sec. VII we summarize the result and discuss its relevance to cross-resistance observed in experiments of bacterial evolution of antibiotic resistance.

II. MODEL

A. Cell model

We adopted a GRN as a model for the cellular state. The GRN is composed of N genes whose expression is represented by the N -dimensional vector $\mathbf{x} = (x_1, x_2, \dots, x_N)$, and the cell state is given by this vector. The time evolution of the state follows the rate equation:

$$\dot{x}_i = f(y_i) - x_i, \quad (1a)$$

$$f(y_i) = \frac{1}{1 + \exp(-y_i)}, \quad (1b)$$

$$y_i = \frac{1}{\sqrt{N}} \sum_{j=1}^N G_{ij} x_j + \frac{1}{N_i} \sum_{j=1}^{N_i} I_{ij} \eta_j + E_i. \quad (1c)$$

\mathbf{G} is an $N \times N$ matrix representing the interactions between genes, satisfying $G_{ij} \in \{-1, 1\}$ ($i \neq j$), $G_{ij} = 0$ ($i = j$). $G_{ij} > 0$ indicates that the product of j th gene positively regulates the i th gene, that is, it accelerates its transcription. $G_{ij} < 0$ represents negative regulation.

$\boldsymbol{\eta}$ is an N_I -dimensional vector that represents the input signal from the external environment to the cell, satisfying $\eta_i \in \{-1, 1\}$. The strength of the interactions between the input signal and the GRN is represented by the $N \times N_I$ matrix \mathbf{I} , satisfying $I_{ij} \in \{-1, 1\}$. \mathbf{E} is an N -dimensional vector representing the environmental stress. In the parametric region used in this study, cellular states always reach a unique fixed point $\mathbf{x}^* = (x_1^*, x_2^*, \dots, x_N^*)$ as a result of time evolution using the rate equation [Eq. (1a)]. In this study we refer to the fixed point \mathbf{x}^* of Eq. (1a) as the phenotype. The phenotype \mathbf{x}^* is uniquely determined for genotype \mathbf{I} , \mathbf{G} and environment $\boldsymbol{\eta}$, \mathbf{E} .

Both terms $\mathbf{I}\boldsymbol{\eta}$ and \mathbf{E} represent the interactions between the external environment and the GRN, but their biological meanings are different. $\mathbf{I}\boldsymbol{\eta}$ represents the signal inputs from the external environment. Such input from the environment appears frequently over long-term, evolutionary timescales, allowing cells to adapt to these environments through evolution. For such evolved cells, we applied environmental stress \mathbf{E} for a laboratory timescale, much smaller than the long-term evolutionary timescale (consider, for instance, the application of antibiotics to wild-type bacteria). Against such inputs, cells may be required to evolve by transient adaptations, which are lost in the long-term evolutionary time scale.

In this model the fitness of a cell is determined by the expression of the output genes, that is, the vector $\mathbf{o} = (o_1, o_2, \dots, o_{N_O})$. The stationary expression of the output genes is given by $o_i^* = f(\sum_{j=1}^N O_{ij}x_j^*/\sqrt{N})$, where \mathbf{O} is an $N_O \times N$ matrix of interactions between the genes in GRN and the target gene, satisfying $O_{ij} \in \{-1, 1\}$. Here we postulate that the fitness for each condition $\boldsymbol{\eta}^{(n)}$ is defined by the negative distance $-|\mathbf{o}^* - \mathbf{t}^{(n)}|^2$ between the output gene expression and the optimal gene pattern $\mathbf{t}^{(n)}$ corresponding to each input signal $\boldsymbol{\eta}^{(n)}$, that is, the fitness takes a maximum value of zero if the expression pattern of the output genes \mathbf{o} matches the optimal gene pattern $\mathbf{t}^{(n)}$ ($n = 0, 1, \dots, P - 1$). Now, we consider P different environmental conditions with input signal $\boldsymbol{\eta}^{(n)}$ ($n = 0, 1, 2, \dots, P - 1$) and an optimal gene pattern $\mathbf{t}^{(n)}$. In this study we consistently use $N = 100$, $N_I = 8$, and $N_O = 8$ [34]

B. Evolution

Evolutionary simulations were performed using the following procedure. In each generation, M mutant cells were created from L mother cells. The total population was ML . Mutant cells were generated by reversing the sign of each matrix element of the genotype \mathbf{I} , \mathbf{G} , \mathbf{O} of the mother cell with probability ρ . In this study, $\rho = 1/N^2 = 0.0001$ was

used. The fitness of each mutant cell was then calculated as follows: We calculated the fixed points \mathbf{x}^* and \mathbf{o}^* using the rate equation (1a) using the four-degree adaptive Runge-Kutta method [35] and used this to calculate the fitness. Initial states for the calculation of the fixed point were randomly chosen from the uniform distribution $0 < x_i < 1$ ($i = 1, 2, \dots, N$). However, because the model adopted in the present study has only one fixed point in the parameter region, the choice of initial values does not affect the results. Finally, the top L fitted cells were selected for the next generation of mother cells. In this study we use $M = 4$ and $L = 25$.

III. EVOLUTIONARY DIMENSION REDUCTION IN THE GENE REGULATORY NETWORK

A. Fitness

First, we performed evolution from randomly generated cells with given matrices \mathbf{I}^{ini} , \mathbf{G}^{ini} and \mathbf{O}^{ini} . \mathbf{I}^{ini} , \mathbf{G}^{ini} , and \mathbf{O}^{ini} are randomly generated with probability p to take ± 1 as follows:

$$p(\mathbf{I}_{ij}^{ini} = \pm 1) = \frac{1}{2}, \quad (2a)$$

$$p(\mathbf{G}_{ij}^{ini} = \pm 1) = \frac{1}{2}, \quad (2b)$$

$$p(\mathbf{T}_{ij}^{ini} = \pm 1) = \frac{1}{2}, \quad (2c)$$

whereas G_{ii} is set to 0.

As mentioned, we assumed that cells need to respond appropriately to external inputs to survive; as such, output genes should take the appropriate expression pattern $\mathbf{t}^{(n)}$ upon input signal $\boldsymbol{\eta}^{(n)}$. Fitness for a input-output pair $(\boldsymbol{\eta}^{(n)}, \mathbf{t}^{(n)})$ under environmental stress \mathbf{E} is given as follows:

$$\mu_n(\mathbf{E}) = - \sum_{i=1}^{N_O} (o_i^*|_{\boldsymbol{\eta}^{(n)}, \mathbf{E}} - t_i^{*(n)})^2, \quad (3)$$

where $\mathbf{o}^*|_{\boldsymbol{\eta}^{(n)}}$ is stationary expression pattern of output genes with input signal $\boldsymbol{\eta}^{(n)}$ and environmental stress \mathbf{E} . Note that $\mu_n(\mathbf{E}) \leq 0$ and $\mu_n(\mathbf{E})$ takes 0 only if the stationary expression pattern of output genes agrees with the target pattern.

In this section, by considering P input-output relationships without environmental stress, that is, $\mathbf{E} = \mathbf{0}$, we used the following fitness function $\bar{\mu}$:

$$\bar{\mu} = \sum_{n=1}^P \mu_n(\mathbf{E} = \mathbf{0}). \quad (4)$$

$\bar{\mu}$ takes a maximum value of 0 only when the output gene expression pattern agrees with the target pattern $\mathbf{t}^{(n)}$ for each of the input signals $\boldsymbol{\eta}^{(n)}$ ($n = 0, 1, \dots, P - 1$) from the environment. In this study we used a nonsignal condition and the following \bar{P} pairs of signals and expression patterns of the output genes (i.e., $P = 2\bar{P} + 1$):

$$\eta_i^{(0)} = 0, \quad t_i^{(0)} = 1/2, \quad (5a)$$

$$\eta_i^{(2m-1)} \in \{-1, 1\}, \quad t_i^{(2m-1)} \in \left\{ \frac{1-2\alpha}{2}, \frac{1+2\alpha}{2} \right\}, \quad (5b)$$

$$\eta_i^{(2m)} = -\eta_i^{(2m-1)}, \quad t_i^{(2m)} = 1 - t_i^{(2m-1)}, \quad (5c)$$

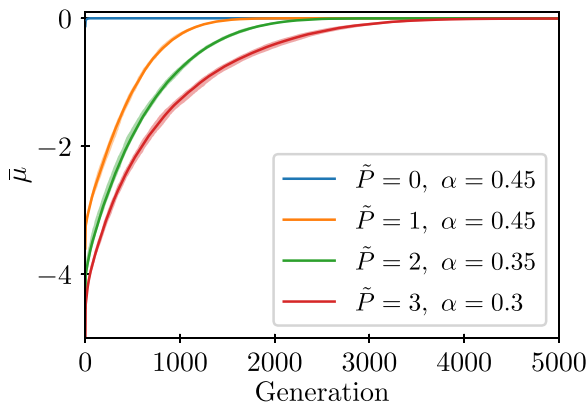


FIG. 1. The evolutionary increase of the given fitness $\bar{\mu}$ averaged over population. Solid lines correspond to the average over 10 independent strains, using different random seed, and the shadows in the background correspond to the range of maximum and minimum values among the 10 strains. The cases ($\tilde{P} = 0, \alpha = 0.45$), ($\tilde{P} = 1, \alpha = 0.45$), ($\tilde{P} = 2, \alpha = 0.35$), and ($\tilde{P} = 3, \alpha = 0.3$) are plotted.

where $m = 1, 2, \dots, \tilde{P}$. Here α is a parameter that represents the strength of the required output gene response, and we define $\alpha^{(m)}$ ($m = 1, 2, \dots, \tilde{P}$) which satisfies $t_i^{(2m)} = (1 + 2\alpha_i^{(m)})/2$. The first signal-target relationship ($\eta^{(0)}, \mathbf{t}^{(0)}$) requires that there is no response to output genes when there are no environmental signals. For $\tilde{P} \geq 1$, we set a pair of patterns $2\tilde{P} - 1$ and $2\tilde{P}$ is symmetric from the case with no input signal. In addition, each input pattern $\eta^{(2m)}$ ($m = 1, 2, \dots, \tilde{P}$) is chosen to be linearly independent. That is, $(\eta^{(2m)} \cdot \eta^{(2m')}) = 0$ ($m \neq m'$). The $\alpha^{(m)}$ ($m = 1, 2, \dots, \tilde{P}$) is equally linearly independent; $(\alpha^{(m)} \cdot \alpha^{(m')}) = 0$ ($m \neq m'$). When a set of $(\eta^{(n)}, \mathbf{t}^{(n)})$ ($n = 0, 1, \dots, 2\tilde{P}$) is given by the above methods, there are linearly independent \tilde{P} signal-target relationships. The purpose of the above pairwise signal-target relationship is to ensure that the symmetry of the phenotypic constraints is obtained as a result of evolution. However, the phenotypic constraints discussed below are obtained even when the signal-target relationship is randomly assigned, without the above symmetry. As a result of evolution, the fitness approached maximum $\bar{\mu} \sim 0$, with $\mu_n(\mathbf{E} = \mathbf{0}) \sim 0$ for $n \leq 2\tilde{P}$, as long as \tilde{P} and α are not so large (Fig. 1). In the following sections, we study the behavior of such evolved networks.

B. Evolutionary dimension reduction

The phenotype of cell \mathbf{x}^* changes when environmental stress \mathbf{E} is imposed. We denote the phenotypic change in response to environmental stress as $\delta\mathbf{x}^*(\mathbf{E}) = \mathbf{x}^*(\mathbf{E}) - \mathbf{x}^*(\mathbf{0})$, where $\mathbf{x}^*(\mathbf{E})$ represents the phenotype of the cell under environmental stress \mathbf{E} , calculated using the environmental signal $\eta^{(0)}$. We calculated phenotypic changes $\delta\mathbf{x}^*(\mathbf{E})$ for cells evolved under various \tilde{P} and α , subjected to 10 000 randomly generated environmental stresses \mathbf{E} . These environmental stresses \mathbf{E} were generated such that each element followed a normal distribution with a mean of 0 and a variance of 1. We investigated the change in phenotype with environmental stress $\delta\mathbf{x}^*(\mathbf{E})$ in the N -dimensional phenotypic space. However, as it is too high-dimensional, we performed prin-

cipal component analysis (PCA) of over 10,000 phenotypic changes $\delta\mathbf{x}^*(\mathbf{E})$ and examined if the variance was explained by a few components. The dependence of the explained variance on \tilde{P} and α is illustrated in Fig. 2.

To study the validity of dimension reduction, we examined the dependence of the explained variance ratio (EVR) on \tilde{P} and α . As shown in Fig. 2(a), the contribution of the top \tilde{P} PCs are large, whereas the components beyond \tilde{P} remain small. Recall that α is a parameter that represents the strength of the required target gene response; the larger α , the larger the response. The top \tilde{P} PCs account for a larger portion of the phenotypic change $\delta\mathbf{x}^*(\mathbf{E})$ than other PCs do. This result implies that \tilde{P} , which represents the number of independent signal-target relationships, determines the dimension of the phenotypic constraint. In contrast to the one-dimensional constraint studied earlier [21,25,36], the constraint to $\tilde{P}(> 1)$ -dimensional constraint is generated, corresponding to the degree of freedom of environmental conditions in which the adaptive evolution progressed [37].

In summary, the dimension of the phenotypic constraint agrees with the degrees of freedom \tilde{P} of the signal-target relationship, and the magnitude of the variance in these directions is correlated with the magnitude of the required target response. Note that the environmental stresses adopted to compute phenotypic variations are not included in the environment where evolution has taken place. However, the response to novel environmental changes is restricted to \tilde{P} -dimensional space after evolution. We also observed this in phenotypic changes caused by genetic mutations in the high-dimensional gene expression space and the corresponding dynamical system analysis for an origin of phenotypic constraint in the dynamical system (see Secs. S1, S2, and S3 in the Supplemental Material [38]). These phenotypic changes due to environmental stresses and genetic mutation are restricted to a common low-dimensional space. This will be important for the correspondence between phenotypic changes in response to environmental stresses and due to adaptive evolution, to be studied in the following sections, including for the formulation of the potential theory in Sec. V.

IV. PREDICTION OF CROSS-RESISTANCE BY PHENOTYPIC CONSTRAINT

A. Fitness

In the previous section, we numerically evolved cells to realize the appropriate target pattern $\mathbf{t}^{(n)}$ ($n = 0, 1, \dots, 2\tilde{P}$) in response to each input signal $\eta^{(n)}$ ($n = 0, 1, \dots, 2\tilde{P}$). As a result, phenotypic changes $\delta\mathbf{x}^*$ in response to environmental stress \mathbf{E} and mutation to genotype \mathbf{G} were constrained to the same subspace with \tilde{P} dimensions.

In this section we adopt cells that have already evolved as in the previous section, achieved the phenotypic constraint, and then studied the evolution of adaptation to novel environmental stresses. This corresponds to the short-term adaptive evolution in laboratory experiments. Using this setup, we computed the cross-fitness, that is, the fitness of a cell that has evolved to adapt to an environmental stress $\mathbf{E}^{(1)}$, exposed to another environmental stress $\mathbf{E}^{(2)}$, and we show that the cross-fitness can be predicted by phenotypic constraints in a low-dimensional subspace.

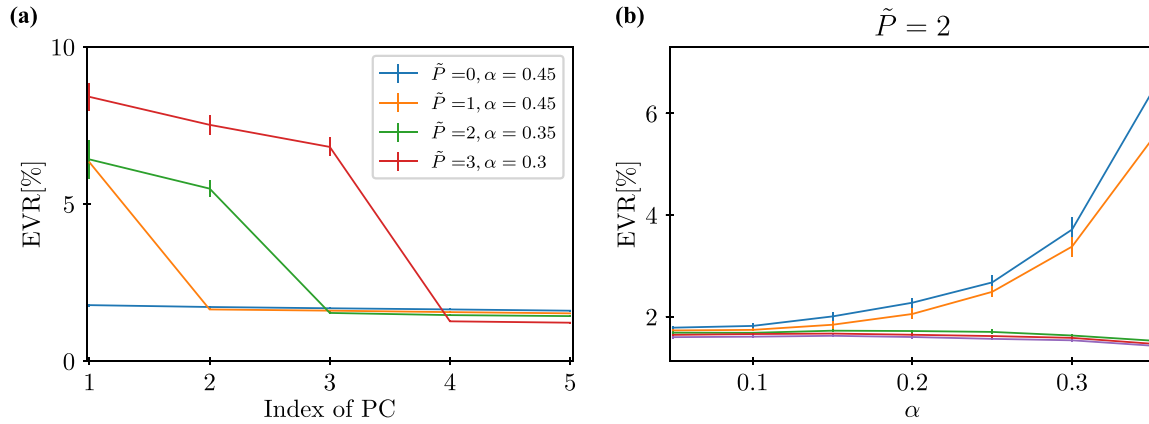


FIG. 2. Explained variance ratio (EVR) of phenotypic changes for the first five principal components (PCs) when random environmental stresses \mathbf{E} generated by $E_i \sim N(0, 1)$ were applied. The changes in \mathbf{x}^* for the evolved gene regulatory network were computed. The phenotypic changes $\delta\mathbf{x}^*(\mathbf{E})$ were obtained for 10 000 independent environmental stresses, from which PCs were computed. (a) The explained variance ratios (EVR) of the PCs of the phenotypic changes of the cell which evolved under different \tilde{P} input-target relationships are plotted. Each explained variance ratio was calculated for the cell with the top fitness value in the population that evolved for $(\tilde{P}, \alpha) = (0, 0.45), (1, 0.45), (2, 0.35), (3, 0.3)$. (b) The explained variance ratios are plotted against the strength of the required target gene response α . Each explained variance ratio was calculated for the cell with the top fitness value in the population that evolved for $\tilde{P} = 1$. The error bars represent the standard deviation of the 10 independent strains. Also see Fig. S1 for the cases $\tilde{P} = 0, 1, 2, 3$ in the Supplemental Material [38].

In this section, we used the fitness $\mu_0(\mathbf{E})$ [see Eq. (3)] in the evolutionary simulations. Evolution with this fitness requires that the appropriate target pattern $\mathbf{t}^{(0)}$ be realized in response to the input signal $\boldsymbol{\eta}^{(0)}$ in the presence of environmental stress \mathbf{E} . Although $\boldsymbol{\eta}^{(0)}$ and $\mathbf{t}^{(0)}$ were used here, the qualitative results did not change when the other pairs of input signals and target gene response patterns were adopted. We calculated the fitness with one input-target relationship, assuming evolution under a constant environment over a short period, such as laboratory evolution.

B. Cross-fitness

Now we introduce the cross-fitness $\mu_{\text{cross}}(\mathbf{E}^{(1)}, \mathbf{E}^{(2)})$, which is defined as the fitness of genotype $\mathbf{G}^*(\mathbf{E}^{(1)})$, that is, the fitness when the cell, which has evolved to adapt to environmental stress $\mathbf{E}^{(1)}$, is exposed to environmental stress $\mathbf{E}^{(2)}$. Thus, it is represented as

$$\mu_{\text{cross}}(\mathbf{E}^{(1)}, \mathbf{E}^{(2)}) = \mu_0(\mathbf{E}^{(2)})_{\mathbf{G}=\mathbf{G}^*(\mathbf{E}^{(1)})}. \quad (6)$$

In other words, the cross-fitness $\mu_{\text{cross}}(\mathbf{E}^{(1)}, \mathbf{E}^{(2)})$ represents the degree of adaptation under environmental stress $\mathbf{E}^{(2)}$ of the cells that evolved to adapt to a different environmental stress $\mathbf{E}^{(1)}$.

In Fig. 3, $\mu_{\text{cross}}(\mathbf{E}^{(1)}, \mathbf{E}^{(2)})$ is plotted as a heat map with the evolved environment $\mathbf{E}^{(2)}$ as the horizontal axis and the environment $\mathbf{E}^{(1)}$ used to measure the fitness as the vertical axis. From the figure, it is difficult to obtain information from the heat map in which the environmental stresses \mathbf{E} are randomly ordered.

To predict cross-fitness, we must find an appropriate feature variable $\mathbf{y}(\mathbf{E})$ that captures the effective internal state corresponding to environmental stress \mathbf{E} . $\mathbf{y}(\mathbf{E})$ is a quantity determined by the cellular state before evolution to adapt to the stress.

Here, as a possible candidate for $\mathbf{y}(\mathbf{E})$, we adopted the PCs of the phenotypic changes $\delta\mathbf{x}^*(\mathbf{E})$ against environmental stress \mathbf{E} for the cells before the evolution because the dominant \tilde{P} PCs capture the phenotypic change under the phenotypic constraint, to which $\delta\mathbf{x}^*(\mathbf{E})$ under environmental stress is restricted. The PC space was calculated using 10 000 random environmental stresses \mathbf{E} , whose elements followed a normal distribution with a mean of 0 and variance of 1. The value $y_i(\mathbf{E})$ is the i th principal component

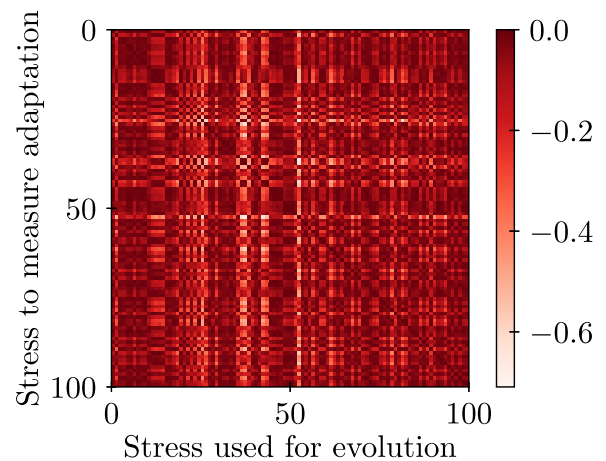


FIG. 3. Fitness when cells evolved under given stress types and are exposed to different stress types. One hundred environmental stress types ($\mathbf{E}^{(1)}, \mathbf{E}^{(2)}, \dots, \mathbf{E}^{(100)}$) were randomly generated. The vertical axis represents the environmental stress used to measure adaptation, and the horizontal axis represents the environmental stress used for evolution. Stresses are ordered by the number of random seeds used to generate environmental stress. Here $y_1^{(i)}$ is the phenotypic change of $\delta\mathbf{x}^{*(i)}$ when environmental stress $\mathbf{E}^{(i)}$ is applied to the cells before evolution.

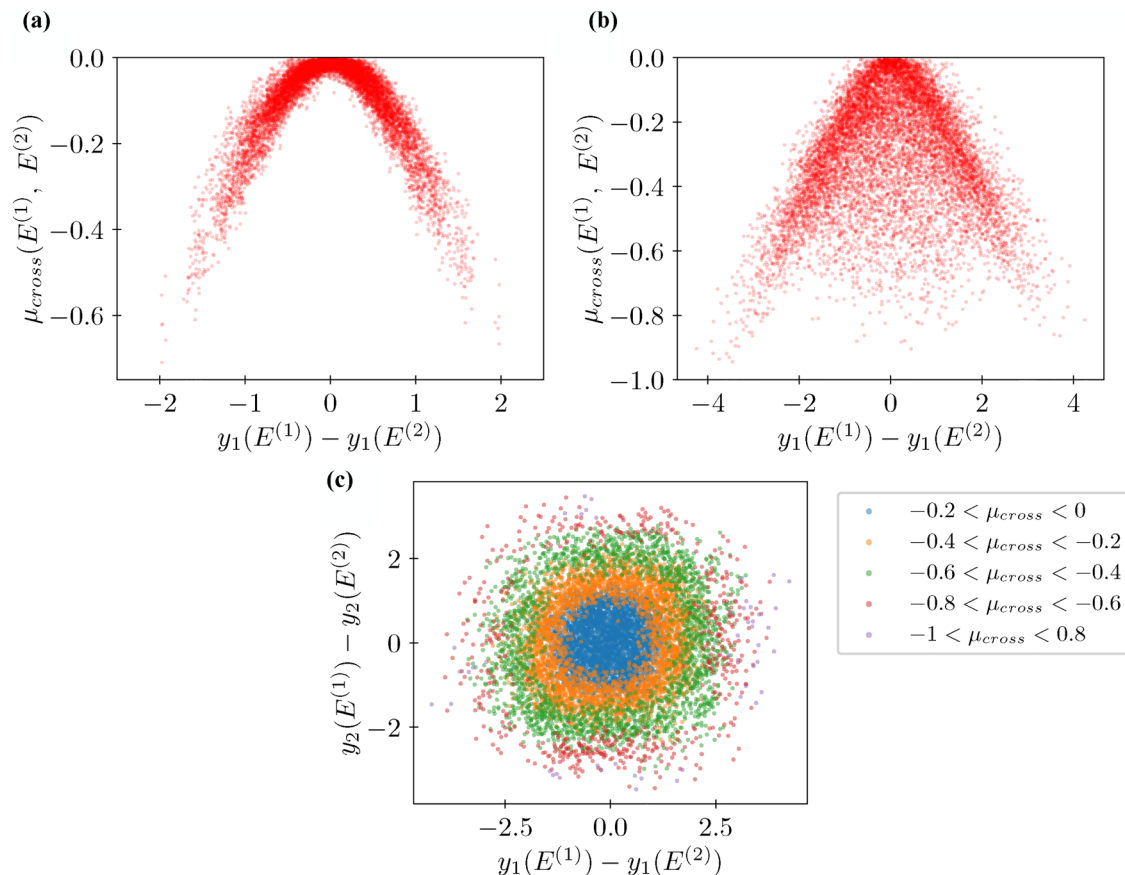


FIG. 4. Cross-fitness $\mu_{\text{cross}}(\mathbf{E}^{(1)}, \mathbf{E}^{(2)})$ is plotted against the difference between the feature values $\mathbf{y}(\mathbf{E}^{(1)}) - \mathbf{y}(\mathbf{E}^{(2)})$ of environmental stress. The feature value $\mathbf{y}(\mathbf{E})$ is the principal component vector of principal component analysis. (a) $\tilde{P} = 1$. The solid lines represent the second-order approximation curve predicted from the theory. The second-order coefficient of the blue line is calculated by the least-squares method from the data on phenotypic changes under 10 000 randomly chosen environmental stresses. The second-order coefficient of the orange line is the $(\partial^2 \mu_0 / \partial y_1^2)$, calculated using the information for the pre-evolutionary genotypes as given in Sec. VB. (b) $\tilde{P} = 2$. When two-dimensional phenotypic constraints exist, we cannot approximate the cross-fitness with the function of a one-dimensional feature value. (c) $\tilde{P} = 2$. The pair of environments $(\mathbf{E}^{(1)}, \mathbf{E}^{(2)})$ used to measure adaptive evolution and cross-adaptation degree is transformed into a two-dimensional feature value space $(y_1(\mathbf{E}^{(1)}) - y_1(\mathbf{E}^{(2)}), y_2(\mathbf{E}^{(1)}) - y_2(\mathbf{E}^{(2)}))$, plotted with colors coded according to the cross-adaptation $\mu_{\text{cross}}(\mathbf{E}^{(1)}, \mathbf{E}^{(2)})$. It can be seen that the pairs of environments corresponding to different adaptations are distributed in a doughnut shape. This is because the cross-fitness $\mu_{\text{cross}}(\mathbf{E}^{(1)}, \mathbf{E}^{(2)})$ at $\tilde{P} = 2$ can be approximated by a monotone univalent function whose arguments are $(y_1(\mathbf{E}^{(1)}) - y_1(\mathbf{E}^{(2)}), y_2(\mathbf{E}^{(1)}) - y_2(\mathbf{E}^{(2)}))$.

value for the phenotypic change $\delta \mathbf{x}^*(\mathbf{E})$. In Fig. 4(a) the cross-fitness $\mu_{\text{cross}}(\mathbf{E}^{(1)}, \mathbf{E}^{(2)})$ across 10 000 random environments is plotted as a function of $y_1(\mathbf{E}^{(1)}) - y_1(\mathbf{E}^{(2)})$ by red dots. It can be seen that the cross-fitness $\mu_{\text{cross}}(\mathbf{E}^{(1)}, \mathbf{E}^{(2)})$ can be approximated by a single curve; that is, the cross-fitness $\mu_{\text{cross}}(\mathbf{E}^{(1)}, \mathbf{E}^{(2)})$ is approximately represented by a single function $\tilde{\mu}_{\text{cross}}(\delta y_1(\mathbf{E}^{(1)}, \mathbf{E}^{(2)}))$ with $\delta y_1(\mathbf{E}^{(1)}, \mathbf{E}^{(2)}) = y_1(\mathbf{E}^{(1)}) - y_1(\mathbf{E}^{(2)})$. This is possible because of the existence of a one-dimensional phenotypic constraint, as we adopted $\tilde{P} = 1$ in this case.

Then, how can cross-fitness be represented for $\tilde{P} = 2$, where the constraint is two-dimensional? Here we show the results for ancestor cells that evolved with $\tilde{P} = 2$ and $\alpha = 0.4$. In Fig. 4(b) we plotted the cross-fitness $\mu_{\text{cross}}(\mathbf{E}^{(1)}, \mathbf{E}^{(2)})$ against $\delta y_1(\mathbf{E}^{(1)}, \mathbf{E}^{(2)})$, similar to Fig. 4(a). In this case, cross-fitness $\mu_{\text{cross}}(\mathbf{E}^{(1)}, \mathbf{E}^{(2)})$ cannot be approximated by a function with a single argument $\delta y_1(\mathbf{E}^{(1)}, \mathbf{E}^{(2)})$. Because the dimension of the phenotype constraint has been increased from 1 to 2,

the cross-fitness $\mu_{\text{cross}}(\mathbf{E}^{(1)}, \mathbf{E}^{(2)})$ is estimated as a function of a two-dimensional PC plane in Fig. 4(c). The difference in the colors of the dots in the figure corresponds to the cross-fitness values. It can be observed that the points with the same cross-fitness are distributed in a doughnut shape in the two-dimensional PC plane. Cross-fitness $\mu_{\text{cross}}(\mathbf{E}^{(1)}, \mathbf{E}^{(2)})$ is represented by a function of two-dimensional arguments $(\delta y_1(\mathbf{E}^{(1)}, \mathbf{E}^{(2)}), \delta y_2(\mathbf{E}^{(1)}, \mathbf{E}^{(2)}))$. It is suggested that when a D -dimensional phenotypic constraint exists, the cross-fitness $\mu_{\text{cross}}(\mathbf{E}^{(1)}, \mathbf{E}^{(2)})$ can be approximated as a function $\tilde{\mu}_{\text{cross}}(\delta y_1, \dots, \delta y_D)$.

In this section, we demonstrate the existence of an approximation function for the cross-fitness. These results suggest that the response of cells to environmental changes and evolution can be linked by phenotypic constraints, from which we can predict the cross-fitness in terms of a few, that is, \tilde{P} , PCs of the phenotypic change before evolution to novel environmental stresses.

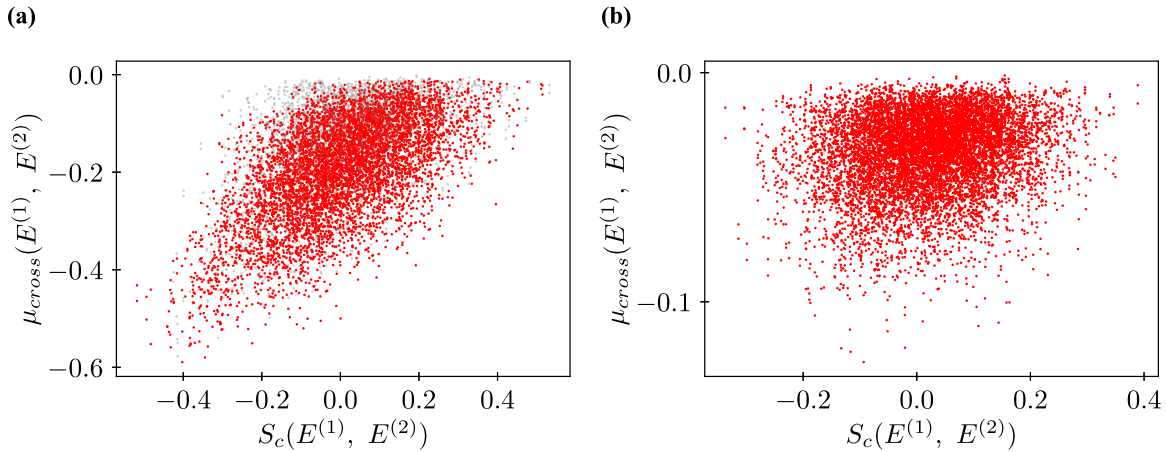


FIG. 5. Cross-fitness is plotted against cosine-similarity. (a) $\tilde{P} = 3$ case with three-dimensional phenotypic constraint. Red dots correspond to the data between pairs of stress environments, under which the magnitude of fitness change was larger than 0.1, whereas gray dots include those smaller than 0.1. The correlation coefficient across all data is 0.57, and that across red dots only is 0.79. (b) $\tilde{P} = 0$ case with no phenotypic constraint. The correlation coefficient is 0.25.

C. Prediction of cross-resistance by cosine similarity

So far we have shown that cross-fitness can be approximated by a single curved surface using the information on the phenotypic constraints of the cell. To obtain this approximation function, information regarding phenotypic constraints, as represented by PCs, is required in advance. However, in a real cell, it may not be easy to determine this information: a large number of PCs are required to provide phenotypic constraints. Here we propose a simpler alternative measure for predicting cross-fitness and demonstrate its reliability using $\tilde{P} = 3$ conditions.

Instead of the difference between the PCs of phenotypic changes in response to environmental stresses, we adopted a simple measure between two phenotypic responses to environmental stresses: cosine similarity for phenotypic change $\delta\mathbf{x}^*(\mathbf{E})$ in response to the stress environment $\mathbf{E}^{(1)}, \mathbf{E}^{(2)}$ defined as follows:

$$S_c(\mathbf{E}^{(1)}, \mathbf{E}^{(2)}) = \frac{[\delta\mathbf{x}^*(\mathbf{E}^{(1)}) \cdot \delta\mathbf{x}^*(\mathbf{E}^{(2)})]}{\|\delta\mathbf{x}^*(\mathbf{E}^{(1)})\| \|\delta\mathbf{x}^*(\mathbf{E}^{(2)})\|}. \quad (7)$$

This is a quantity characterizing orientations between phenotypic changes $\delta\mathbf{x}^*(\mathbf{E}^{(1)})$ and $\delta\mathbf{x}^*(\mathbf{E}^{(2)})$; it takes 1 if they are oriented in the same direction, -1 if they are oriented in the exact opposite direction, and 0 if they are uncorrelated [39]. The cosine similarity is symmetric for the stress environments $\mathbf{E}^{(1)}$ and $\mathbf{E}^{(2)}$.

In Fig. 5(a) the cross-fitness is plotted against cosine-similarity across the pairs of randomly generated environments (both red and gray points). For $\tilde{P} = 3$, one can see the correlation between cross-fitness and cosine similarity (correlation coefficient 0.57). However, the correlation might not be significant, as shown in Fig. 5(a). The main reason for this is that for some stresses \mathbf{E} , the response is rather small, so the cosine similarity and fitness change are small. To eliminate such “nonresponse” cases, we replotted the data across only the environment pairs under which the fitness decrease was larger than 0.1 [red dots in Fig. 5(a)], for which the correlation coefficient was 0.79. It should be noted that, in this

case, it is difficult to see clearly discernible few-dimensional structure as in Figs. 4(a) and 4(b) [also see Supplemental figure Fig. S5(a) [38] for the case $\tilde{P} = 3$]. Still, we get the correlation as in Fig. 5(a).

The prediction of cross-fitness using cosine similarity does not require direct information on phenotypic constraints. However, such constraints are necessary for the correlation between cross-fitness and cosine similarity. Owing to the low-dimensional constraint, the environmental and evolutionary responses are correlated in the low-dimensional space, which reflects the cosine similarity (see also the discussion in the next section). For $\tilde{P} = 0$, in which no phenotypic constraints evolved as no input-output relationship was postulated, such a correlation was not observed [Fig. 5(b), correlation coefficient 0.25].

V. REPRESENTATION OF CROSS-FITNESS BY FITNESS POTENTIAL FUNCTION

A. Potential approximation of cross-fitness in low-dimensional phenotype space

In the previous section, we showed that cross-fitness can be approximated based on the information that the phenotypic response of cells to environmental stresses is constrained in low-dimensional space. In this section we describe a potential theory that characterizes the phenotypic response by representing fitness as a function of environmental and genetic changes. This theory demonstrates that the result on the cross-resistance does not depend on the specific choice of the models, but is universal as long as the phenotypic changes are constrained into a much lower dimensional manifold than an original degree of freedom N .

For this, we consider a fitness function $u(\mathbf{X})$ of D -dimensional variable $\mathbf{X} = (X_1, X_2, \dots, X_D)$. \mathbf{X} is given as a function of genotype \mathbf{G} and environment \mathbf{E} . When phenotypic constraints exist, the phenotypic changes caused by environmental stress and genotypic mutations are restricted to a low, D -dimensional submanifold within the total N -dimensional phenotypic space. Here D is not necessarily one or few, but

the assumption that D is $o(N)$ is necessary for macroscopic potential description.

We assume that the fitness function $u(X(\mathbf{G}, \mathbf{E}))$ has a maximum value at $\mathbf{G}^{(0)}, \mathbf{E}^{(0)}$. This means that the cell with genotype $\mathbf{G}^{(0)}$ is adapted to environment $\mathbf{E}^{(0)}$. By expanding the fitness function $u(X(\mathbf{G}, \mathbf{E}))$ around $\mathbf{G} = \mathbf{G}^{(0)}, \mathbf{E} = \mathbf{E}^{(0)}$ up to the second order, we obtain the following:

$$u \simeq u_0 + \delta u^{(2)}, \quad (8a)$$

$$u_0 = u(X(\mathbf{G}^{(0)}, \mathbf{E}^{(0)})), \quad (8b)$$

$$\delta u^{(2)}(\delta \mathbf{X}) = \frac{1}{2} \sum_{i,j=1}^D \frac{\partial^2 u}{\partial X_i \partial X_j} \delta X_i \delta X_j, \quad (8c)$$

$$\begin{aligned} \delta X_i(\delta \mathbf{G}, \delta \mathbf{E} | \mathbf{G}^{(0)}, \mathbf{E}^{(0)}) &= \delta X_i^G(\delta \mathbf{G} | \mathbf{G}^{(0)}, \mathbf{E}^{(0)}) \\ &+ \delta X_i^E(\delta \mathbf{E} | \mathbf{G}^{(0)}, \mathbf{E}^{(0)}), \end{aligned} \quad (8d)$$

where $\delta X_i^G(\delta \mathbf{G} | \mathbf{G}^{(0)}, \mathbf{E}^{(0)}) = [\partial X_i / \partial \mathbf{G}]_{\mathbf{E}=\mathbf{E}^{(0)}}^{G=\mathbf{G}^{(0)}} \cdot \delta \mathbf{G}$ with $\delta \mathbf{G} = \mathbf{G} - \mathbf{G}^{(0)}$ and $\delta X_i^E(\delta \mathbf{E} | \mathbf{G}^{(0)}, \mathbf{E}^{(0)}) = [\partial X_i / \partial \mathbf{E}]_{\mathbf{E}=\mathbf{E}^{(0)}}^{G=\mathbf{G}^{(0)}} \cdot \delta \mathbf{E}$ with $\delta \mathbf{E} = \mathbf{E} - \mathbf{E}^{(0)}$. Unless otherwise noted, $\delta X_i(\delta \mathbf{G}, \delta \mathbf{E} | \mathbf{G}^{(0)}, \mathbf{E}^{(0)})$ will be denoted as $\delta X_i(\delta \mathbf{G}, \delta \mathbf{E})$ without $(\mathbf{G}^{(0)}, \mathbf{E}^{(0)})$; similarly for other variables. Recall that the condition \mathbf{E} in Secs. III and IV denotes the environmental changes from the original state and thus corresponds to $\delta \mathbf{E}$ in this section.

Note that the first-order derivatives $(\partial u / \partial \mathbf{X})$ is equal to $\mathbf{0}$, because the fitness function reaches a (local) maximum at $X(\mathbf{G}^{(0)}, \mathbf{E}^{(0)})$. Fitness generally decreases with an environmental change $\delta \mathbf{E}$; however, it is recovered by the changes in the genotype \mathbf{G} with the evolution. At the end of the evolution, the fitness reaches a local maximum at $X(\mathbf{G}^*(\mathbf{E}), \mathbf{E})$. Hence, $\mathbf{G}^*(\mathbf{E})$ should satisfy the following condition [40]:

$$\mathbf{G}^*(\mathbf{E}) \in \operatorname{argmax}_{\mathbf{G}} [u(X(\mathbf{G}, \mathbf{E}))]. \quad (9)$$

Rewriting Eq. (9) using the potential approximation of the fitness function [Eq. (8c)], we get $\delta \hat{\mathbf{G}}^*(\delta \mathbf{E}) = \hat{\mathbf{G}}^*(\mathbf{E}) - \mathbf{G}^{(0)}$, where $\hat{\mathbf{G}}^*(\mathbf{E})$ is second-order approximation for $\mathbf{G}^*(\mathbf{E})$, as

$$\delta \hat{\mathbf{G}}^*(\delta \mathbf{E}) \in \operatorname{argmax}_{\delta \mathbf{G}} \left[\sum_{i,j=1}^D \frac{\partial^2 u}{\partial X_i \partial X_j} \delta X_i \delta X_j \right]. \quad (10)$$

Because the fitness function takes the maximum value at $\mathbf{G}^{(0)}, \mathbf{E}^{(0)}$, all eigenvalues of the matrix $\mathbf{H} = \{H_{ij} = (\partial^2 u / \partial X_i \partial X_j)_{\mathbf{G}^{(0)}, \mathbf{E}^{(0)}}\}$ are negative, and \mathbf{H} satisfies $\mathbf{x}^T \mathbf{H} \mathbf{x} \leq 0$ for any vector \mathbf{x} , and $\mathbf{x}^T \mathbf{H} \mathbf{x}$ takes 0 and only under the condition $\mathbf{x} = \mathbf{0}$ [we assume that the change by stress is not so large, and remains within the range of the linear approximation in Eq. (8a) is valid]. Therefore, when fitness is completely recovered by the genotype change $\mathbf{G}^{(0)} \rightarrow \hat{\mathbf{G}}^*(\mathbf{E})$, $\delta \mathbf{X}(\delta \hat{\mathbf{G}}^*(\delta \mathbf{E}), \delta \mathbf{E})$ should be a zero vector. Then the following relationship holds:

$$\delta X_i^G(\delta \hat{\mathbf{G}}^*(\delta \mathbf{E})) = -\delta X_i^E(\delta \mathbf{E}) \quad (i = 1, 2, \dots, D). \quad (11)$$

The conditions Eq. (11) indicate that the phenotypic changes caused by environmental change $\mathbf{E}^{(0)} \rightarrow \mathbf{E}$ are canceled out by genetic changes $\mathbf{G}^{(0)} \rightarrow \hat{\mathbf{G}}^*(\mathbf{E})$ [justification of Eq. (11) in the evolution simulation is discussed in the Appendix].

When the conditions Eq. (11) are satisfied, then Eq. (8c) with $\hat{\mathbf{G}}^*(\mathbf{E}^{(1)})$ and $\mathbf{E}^{(2)}$ can be written as follows:

$$\delta u^{(2)} = \frac{1}{2} \sum_{i,j} \frac{\partial^2 u}{\partial X_i \partial X_j} \delta X_i' \delta X_j', \quad (12a)$$

$$\delta X_i'(\delta \mathbf{E}^{(1)}, \delta \mathbf{E}^{(2)}) = \delta X_i^E(\delta \mathbf{E}^{(1)}) - \delta X_i^E(\delta \mathbf{E}^{(2)}). \quad (12b)$$

This equation implies that the fitness of the cell that has evolved under environment $\mathbf{E}^{(1)}$, placed in environment $\mathbf{E}^{(2)}$, is given as a function of the difference between the phenotypic changes $\delta \mathbf{X}^E(\delta \mathbf{E})$ under environment changes $\delta \mathbf{E}^{(1)}$ and $\delta \mathbf{E}^{(2)}$. In Sec. IV B, the change $\delta \mathbf{X}^E$ in Eq. (12a) is given by the changes in the PCs. Then cross-fitness $\mu_{\text{cross}}(\mathbf{E}^{(1)}, \mathbf{E}^{(2)}) = \mu_0(\mathbf{E}^{(2)})$ with $\mathbf{G} = \mathbf{G}^*(\mathbf{E}^{(1)})$ can be approximated as a function of $\mathbf{y}(\mathbf{E}^{(1)}) - \mathbf{y}(\mathbf{E}^{(2)})$; the difference in the PC changes in the phenotypes between $\mathbf{E}^{(1)}$ and $\mathbf{E}^{(2)}$.

B. Application of potential theory to the result of evolution simulation

Following the argument in the last section, we estimate the coefficient of the second term of the cross-fitness $(\partial^2 \mu_{\text{cross}} / \partial y_1^2)$ (y_1 is the first PC of the phenotypic change $\delta \mathbf{x}^*$) from the change in μ_{cross} against the change in y_1 . The solid lines in Fig. 4 are predicted curves according to the above theory for $\bar{P} = 1$ and $\alpha = 0.45$. The coefficient of the blue one is calculated by the least-squares method with $\mu_{\text{cross}} = -cy_1^2$ changing c . This curve approximates cross-fitness well, especially in regions where phenotypic changes are not too large.

Next, we interpret the relationship between cosine similarity and cross-fitness in Fig. 5(a) with the potential theory. By expanding $\delta X_i'$, Eq. (12a) can be rewritten as

$$\begin{aligned} \delta u^{(2)} &= \frac{1}{2} \sum_{i,j} \frac{\partial^2 u}{\partial X_i \partial X_j} \delta X_i^E(\delta \mathbf{E}^{(1)}) \delta X_j^E(\delta \mathbf{E}^{(1)}) \\ &+ \frac{1}{2} \sum_{i,j} \frac{\partial^2 u}{\partial X_i \partial X_j} \delta X_i^E(\delta \mathbf{E}^{(2)}) \delta X_j^E(\delta \mathbf{E}^{(2)}) \\ &- \sum_{i,j} \frac{\partial^2 u}{\partial X_i \partial X_j} \delta X_i^E(\delta \mathbf{E}^{(1)}) \delta X_j^E(\delta \mathbf{E}^{(2)}). \end{aligned} \quad (13)$$

The first and second terms in the above equation can then be interpreted as second-order approximations of fitness changes under stress environments $\mathbf{E}^{(1)}$ and $\mathbf{E}^{(2)}$. The third term represents the interaction between stress environments $\mathbf{E}^{(1)}$ and $\mathbf{E}^{(2)}$, that is, the fitness change in $\mathbf{E}^{(2)}$ owing to adaptive evolution under $\mathbf{E}^{(1)}$. This term is proportional to the inner product of the phenotypic changes $\delta \mathbf{X}^E(\delta \mathbf{E}^{(1)})$ and $\delta \mathbf{X}^E(\delta \mathbf{E}^{(2)})$ under the metric $\mathbf{H} = \{\partial^2 u / \partial X_i \partial X_j |_{\mathbf{G}^{(0)}, \mathbf{E}^{(0)}}\}$. In other words, the third term corresponds to the difference in the orientation of phenotypic changes in $\mathbf{E}^{(1)}$ and $\mathbf{E}^{(2)}$, the similarity between the environments. In particular, when the first and second terms take the same value (fitness changes in $\mathbf{E}^{(1)}$ and $\mathbf{E}^{(2)}$ are the same), the cross-fitness is proportional to the cosine similarity under the metric \mathbf{H} . This proportional relationship between cross-fitness and cosine similarity supports the results presented in Sec. IV C. Note that this relationship is obtained because the Hessian matrix of the cross-fitness can

be approximated well by a constant multiple of the unit matrix in the present model.

VI. APPLICATION FOR LABORATORY EVOLUTION OF RESISTANCE TO ANTIBIOTICS

In this section we apply the present theory to the experimental evolution of antibiotic resistance in *E. coli*, to confirm the prediction of cross-fitness by transcriptome changes. For details of the experiment evolution, see Sec. VIII and [8].

Here six antibiotics—cefoperazone (CPZ), cefixime (CFIX), amikacin (AMK), neomycin (NM), enoxacin (ENX), and ciprofloxacin (CPFX)—were used for the experimental evolution, which is below denoted as $A^{(1)}, A^{(2)}, \dots, A^{(6)}$, respectively. In this experiment, the condition without the addition of antibiotics corresponds to $E^{(0)}$ in Sec. V, and the addition of antibiotics corresponds to environmental change δE . First, each antibiotic $A^{(k)}$ was added to the parental strain up to the level as long as the growth is sustained. This level is called the minimum inhibitory concentration (MIC), which is the lowest concentration of an antibiotic that prevents visible bacterial growth and is used as a measure to quantify antibiotic resistance, which corresponds to the fitness here. As a measure of phenotypic changes, we used log-transformed transcriptome responses, following our previous study [21], because changes in gene expression typically occur on the logarithmic scale. Namely, the phenotypic change was measured by the transcriptome change as $\delta X_i(A^{(k)}) = \log_2[x_i(A^{(k)})/x_i(ND)]$, where $x(A^{(k)})$ is the transcriptome data when an antibiotic $A^{(k)}$ is added near the MIC to the parent strain before evolution and $x(ND)$ is the geometric mean of three independently measured transcriptome data under no-drug condition. As the fitness measure, we used log-transformed MIC values $[\log_2(\mu\text{g/ml})]$ based on the previous study [8], which showed a linear correlation between log-transformed transcriptome changes and log-transformed MIC values. As MIC is larger, the fitness under the antibiotic is larger, so the former can be used as a measure of fitness. Assuming that the laboratory evolution results in complete adaptation to antibiotics, we computed the relative MIC $R_{MIC}(A^{(k)}, A^{(l)}) = MIC(A^{(k)}, A^{(l)}) - MIC(A^{(l)}, A^{(l)})$, where $MIC(A^{(k)}, A^{(l)})$ is the log-transformed MIC for $A^{(l)}$ of the strain that evolved to be resistant to $A^{(k)}$, and used it as the measure of cross-fitness [41]. This quantity is nonpositive, which takes zero when $A^{(k)}$ and $A^{(l)}$ are the same antibiotics.

Next, similarly to Sec. IV C, we computed the differences $y_1(A^{(k)}) - y_1(A^{(l)})$ of the first principal component for an antibiotic $A^{(k)}$ used for the evolution of resistance and antibiotics $A^{(l)}$ used to measure the resistance of the evolved strain. In Fig. S5(b) [38], we plotted the measure of cross-fitness $R_{MIC}(A^{(k)}, A^{(l)})$ against $y_1(A^{(k)}) - y_1(A^{(l)})$. A clear one-dimensional curve was not observed as in Fig. S5(a) [38]. Hence, the phenotypic changes were not constrained in a one-dimensional space.

Note, however, that the potential theory does not require the reduction to one or two or three dimensions, but postulated only the reduction to $O(1)$ (i.e., much smaller than N , say, 10 [8]). Accordingly, it will be legitimate to compare the experimental data with the prediction of the theory. Hence, we then plotted the correlation between $R_{MIC}(A^{(k)}, A^{(l)})$ and

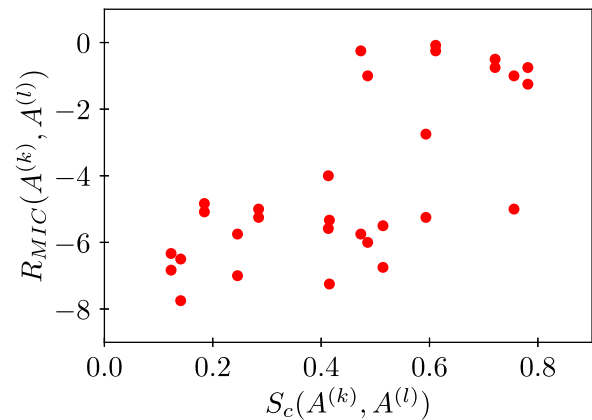


FIG. 6. Relative MIC $R_{MIC}(A^{(k)}, A^{(l)})$ $[\log_2(\mu\text{g/ml})]$ are plotted against cosine similarity $S_c(A^{(k)}, A^{(l)})$. $S_c(A^{(k)}, A^{(l)})$ is defined as $S_c(A^{(k)}, A^{(l)}) = (\delta X(A^{(k)}) \cdot \delta X(A^{(l)})) / |\delta X(A^{(k)})| |\delta X(A^{(l)})|$. Pearson's correlation coefficient is 0.70, and the p value is 1.5×10^{-5} .

the cosine similarity $S_c(A^{(k)}, A^{(l)})$ (Fig. 6), which corresponds to Fig. 5(a). The data showed a significant correlation between them (Pearson's correlation coefficient is 0.70 with a p value of 1.5×10^{-5}). Recalling that the gene expression dynamics involve hundreds of genes, this value is remarkable. Indeed, it is about a similarly high value as obtained from the simulation for $\tilde{P} = 3$. This result indicates that the present theory applies to the laboratory evolution of resistance to antibiotics.

VII. DISCUSSION

In the present study, we first evolved the gene regulatory network to be capable of multiple input-output relationships, to demonstrate that phenotypic changes due to environmental stress and genetic mutations are constrained to a lower-dimensional subspace, whose dimension corresponds to the degrees of freedom of the input-output relationship required for fitness. Phenotypic changes due to environmental stress and genotypic mutation are constrained to the common subspace, as formulated by dynamical system theory (see also [24,26,36,42–47] for the relevance of dimensional reduction in biological systems).

In the present GRN model, phenotypic constraints were caused by the separation of \tilde{P} eigenvalues. The dominant phenotypic changes owing to environmental changes and genetic mutations are constrained in the directions of the eigenvectors of these eigenvalues. Then we conducted evolutionary simulations under stress environments $E^{(k)}$ using the evolved GRN exhibiting phenotypic constraints as the ancestor cell. We defined the cross-fitness $\mu_{\text{cross}}(E^{(1)}, E^{(2)})$ as fitness of the cells evolved in the stress environment $E^{(1)}$ in the stress environment $E^{(2)}$. We then demonstrated that this cross-fitness is represented by the \tilde{P} -dimensional PC of the phenotypic change $\delta x^*(E^{(1)})$ and $\delta x^*(E^{(2)})$, cellular state changes to each stress E , before the evolution to stress. Thus, the cross-fitness $\mu_{\text{cross}}(E^{(1)}, E^{(2)})$ can be well represented by low-dimensional (\tilde{P}) phenotypic variables. This indicates that the fitness of the stress environment can be predicted by measuring the phenotypic changes in pre-evolutionary cells by the application of environmental stress.

To quantitatively formulate the cross-fitness observed in evolutionary simulations, we introduced the fitness potential. The decrease in fitness due to stress is recovered when the phenotypic change in evolution completely cancels out the phenotypic change due to the stressful environment. By using the potential theory, cross-fitness can be approximated by the difference in phenotypic responses to the stress used for the evolution and that applied later for the test. Note that the potential theory works as long as the phenotypic changes are constrained to a low-dimensional manifold compared to the number of protein/mRNA species. Thus, simulation results are supported, but furthermore the theory demonstrated the generality of the results, independent of the details of the model.

In this potential approximation, the cross-fitness is symmetric against $\mathbf{E}^{(1)}$ and $\mathbf{E}^{(2)}$, that is, $\mu_{\text{cross}}(\mathbf{E}^{(1)}, \mathbf{E}^{(2)}) = \mu_{\text{cross}}(\mathbf{E}^{(2)}, \mathbf{E}^{(1)})$. Note that this is obtained by expanding the fitness up to the second order of phenotypic changes due to environmental changes and genetic mutations by assuming that these are not very large. If perturbations are much larger, the third- or higher-order effects are not negligible, and the above symmetry no longer holds. However, even if the cross-fitness is not symmetric, it is expected to correlate with the cosine similarity (which is symmetric by definition) to a sufficient degree.

The potential theory considered in this paper assumes the existence of a low-dimensional structure in which phenotypic changes due to environmental responses and mutations are constrained. If such a low-dimensional structure did not exist, phenotypic changes in evolution would be extremely random, and it would not be possible to make the predictions of evolution discussed in this paper.

Notably, in the model in the present study, the Euclidian distance between the expression pattern of the output gene and the target pattern is used as the fitness function, which is symmetric for the input-output relationship ($\eta^{(0)}, \epsilon^{(0)}$). This symmetry eliminates the third-(or odd-) order terms in the potential form. Hence, the symmetry could be violated to some degree, depending on the choice of the input-output relationship and fitness function.

Finally, we discuss the applications of our theory to experimental studies on laboratory evolution. In the present study, we first discuss the prediction of cross-fitness using the PCs of phenotypic changes in response to environmental change. To do this, information on the representation of the fitness by the PCs is needed in addition to information on phenotypic constraints, which may not be obtained directly from experimental data. Later, however, we demonstrated the correlation between cross-fitness and cosine similarity in phenotypic changes in response to the stressful environment. Indeed, the previous experimental data [8] suggest that transcriptome changes of laboratory evolution of *E. coli* were not constrained to one or two dimensions, but still restricted at low dimension at around 10. Hence, it is valid to apply the potential theory, and accordingly the cross-fitness after evolution could be predicted by the transcriptome changes due to antibiotics before evolution (Sec. VI).

In the potential theory in the present study, we focused only on the full recovery of fitness via adaptive evolution in a stressful environment. However, in actual evolution, fitness

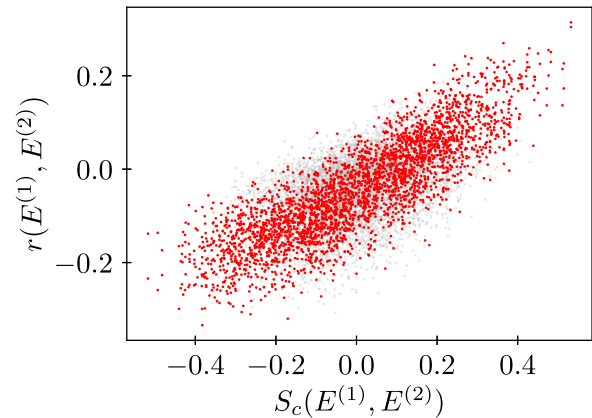


FIG. 7. Cross-resistance is plotted against cosine similarity for $\tilde{P} = 3$ case with three-dimensional phenotypic constraint. Red dots represent the data from the stress environment, under which fitness change is larger than -0.1 . Gray dots represent data with smaller fitness changes. The correlation coefficient across all data is 0.69, and that across only red dots is 0.85.

may not be fully restored. We expect that our study will still provide relevant information in such cases, as long as phenotypic constraint exists and evolution occurs along it under a given fitness landscape. However, when a single mutation introduces drastic phenotypic changes or strong epistasis occurs during evolution, the correlation between cross-fitness and transcriptome cosine similarity may not be clearly observed.

In the present study, long-term evolution provided a phenotypic constraint to the cellular state, and later adaptive evolution of such cells to a stress environment follows the already created constraint. This implicitly assumes that there is a timescale gap between the evolution of the present cells and their laboratory evolution to gain stress tolerance. The phenotypic constraint itself was shaped by the former evolutionary process but was not altered by the later, shorter-term evolutionary process.

Thus far, we have discussed cross-fitness in the presence of phenotypic constraints. Another commonly adopted measure of relative changes by evolution and adaptation is cross-resistance $r(\mathbf{E}^{(1)}, \mathbf{E}^{(2)})$, given by

$$r(\mathbf{E}^{(1)}, \mathbf{E}^{(2)}) = \mu_{\text{cross}}(\mathbf{E}^{(1)}, \mathbf{E}^{(2)}) - \mu_{\text{cross}}(\mathbf{0}, \mathbf{E}^{(2)}). \quad (14)$$

It is defined as cross-fitness between $\mathbf{E}^{(1)}$ and $\mathbf{E}^{(2)}$ minus the fitness of the pre-evolutionary cell because we are mostly concerned with the relative fitness changes as a result of adaptive evolution. Therefore, even if the cross-fitness is symmetric, as in the present model, cross-resistance is not. We should note this point when applying the present theory to cross-resistance using Eq. (14). Still, the present theory can be used to predict the cross-resistance (see Fig. 7) for an example of the correlation between cross-resistance and transcriptome cosine similarity. This quantity is usually used as a measure to quantify antibiotic resistance. This will be useful for experimental verification of the present theory.

VIII. MATERIALS AND METHODS

We describe the method of laboratory evolution and the acquisition of data used in Sec. VI. The insertion

sequence-free *Escherichia coli* strain MDS42 [48] was purchased from Scarab Genomics. The cells were cultured in 200 μl modified M9 medium [49] in 96-well microplates with shaking at 900 strokes min^{-1} at 34 $^{\circ}\text{C}$. We prepared precultures by shaking -80°C glycerol stocked MDS42 strains for 23 h without antibiotics. The cells precultured were diluted to an $\text{OD}_{600\text{ nm}}$ of 1×10^{-4} into 200 μl of fresh modified M9 medium in 96-well microplates with and without antibiotics. The final concentrations of antibiotics used in this study were as follows; 3.9×10^{-3} $\mu\text{g}/\text{ml}$ for cefoperazone (CPZ), 1.2×10^{-2} $\mu\text{g}/\text{ml}$ for Cefixime (CFIX), 4.0 $\mu\text{g}/\text{ml}$ for amikacin, 2.0 $\mu\text{g}/\text{ml}$ for neomycin (NM), 3.1×10^{-2} $\mu\text{g}/\text{ml}$ for enoxacin (ENX), and 2.0×10^{-3} $\mu\text{g}/\text{ml}$ for ciprofloxacin (CPFX), respectively. The cultures were grown to an $\text{OD}_{600\text{ nm}}$ in the 0.072–0.135 range (the equivalent of 10 generations). Next 180 μl of exponential cultures were withdrawn rapidly, and cells were killed immediately by the addition of an equal volume of ice-cold ethanol that contained 10% (w/v) phenol. The cells were collected by centrifugation at $20\,000 \times g$ at 4 $^{\circ}\text{C}$ for 5 min, and the pelleted cells were stored at -80°C prior to RNA extraction. Total RNA was isolated and purified from cells using RNeasy micro Kit with on-column DNA digestion (Qiagen) in accordance with the manufacturer's instructions.

Transcriptome analysis was performed as in a previous study [8] using a custom-designed Agilent $8 \times 60\text{ K}$ array for *E. coli* W3110. Briefly, 100 ng of each purified total RNA sample was labeled using the Low Input Quick Amp WT Labeling kit (Agilent Technologies) with cyanine3 (Cy3) according to the manufacturer's instructions. Cy3-labeled cRNAs were fragmented and hybridized to the microarray for 17 h at 65 $^{\circ}\text{C}$ in a hybridization oven. Washing and scanning of microarrays were performed in accordance with the manufacturer's instructions. Microarray image analysis was performed using Feature Extraction version 10.7.3.1 (Agilent Technologies).

The MIC values of evolved *E. coli* strains for the aforementioned six antibiotics were obtained in the previous study [8]. The transcriptome data and MIC values are available upon request.

In the data analysis, the intensity values were normalized using the quantile normalization method. We then excluded the following genes which the parent strain lacks: *fluA*, *yagE*, *yagF*, *yagG*, *yagM*, *yagX*, *appY*, *ycdR*, *yfmD*, *yfmJ*, *ycgG*, *paal*, *ydbD*, *cheW*, *yfjL*, *yqiG*, *yqiL*, *yhhZ*, *yrhA*, *intB*, *yjhl*, *fimD*, *hsdR*, and *yjiY*. Furthermore, we excluded genes with low expression levels (≤ 100 a.u. in any strain) and with relatively small expression change in response to all six antibiotics ($\delta X_i(A^{(k)}) = \log_2[x_i(A^{(k)})/x_i(ND)] \leq 1$ for all $A^{(k)}$), since the expression changes of such low expression or relatively unchanged genes were dominated by the experimental errors.

Source codes for the evolutionary simulations are openly available from the GitHub [50].

ACKNOWLEDGMENTS

We thank Tetsuhiro Hatakeyama for his insightful comments. This research was partially supported by a Grant-in-Aid for Scientific Research (A) (20H00123), a Grant-in-Aid for Scientific Research on Innovative Areas (17H06386) from

the Ministry of Education, Culture, Sports, Science and Technology (MEXT) of Japan, the Japan Society for the Promotion of Science (20J12168), and the Japanese Science and Technology agency (JST) ERATO (JPMJER1902). This research was also supported by the Novo Nordisk Foundation (NNF 0065542).

APPENDIX: COSINE SIMILARITY BETWEEN PHENOTYPIC CHANGES DUE TO ENVIRONMENTAL STRESS AND GENETIC CHANGES THROUGH ADAPTIVE EVOLUTION

In Sec. V we assumed that phenotypic changes due to environmental changes would be completely canceled out by phenotypic changes due to genotypic changes through evolution. To test that this assumption held in the evolutionary simulations, we measured the cosine similarity between phenotypic changes against environmental stress and the evolution under it:

$$S_c(\mathbf{E}) = \frac{[\delta \mathbf{x}_{env}^*(\mathbf{E}) \cdot \delta \mathbf{x}_{evo}^*(\mathbf{E})]}{\|\delta \mathbf{x}_{env}^*(\mathbf{E})\| \|\delta \mathbf{x}_{evo}^*(\mathbf{E})\|}, \quad (\text{A1})$$

where $\delta \mathbf{x}_{evo}^*(\mathbf{E})$ is the phenotypic change in response to environmental stress \mathbf{E} and $\delta \mathbf{x}_{env}^*(\mathbf{E})$ is the phenotypic change from evolution with environmental stress \mathbf{E} .

The potential theory discussed in this section assumes the ideal limit in which the phenotypic change $\delta \mathbf{x}_{evo}^*(\mathbf{E})$ due to genotypic change will completely cancel out the phenotypic change $\delta \mathbf{x}_{env}^*(\mathbf{E})$ due to environmental change, thereby recovering the fitness. The histogram shown in blue in Fig. 8(a) represents the genotypes that evolved at $\tilde{P} = 0$, $\alpha = 0.45$. In this case there are no phenotypic constraints, and the histogram does not deviate from the peak at similarity ~ 0 . In contrast, the histogram plotted in orange represents the data examined for adaptive evolution from genotypes that evolved at $\tilde{P} = 1$, $\alpha = 0.45$, where a one-dimensional phenotypic constraint is achieved. The distribution of cosine similarity is extended into negative regions, as shown in Fig. 8(a). This implies that, when phenotypic constraints are present, the increased proportion of evolved cells has a cosine similarity closer to -1 . The closer the cosine similarity is to -1 , the more the phenotypic change $\delta \mathbf{x}_{evo}^*(\mathbf{E})$ in adaptive evolution is correlated with the phenotypic change $\delta \mathbf{x}_{env}^*(\mathbf{E})$ in response to environmental change.

To investigate how a larger proportion of evolution leads to cosine similarity close to -1 , the histograms in the presence of one-dimensional phenotypic constraints were computed separately according to fitness when the pre-evolutionary cells were subjected to environmental stresses. As plotted in Fig. 8(b), the cosine similarity, as a result of evolution against environmental stresses, shifted to a negative value, heading towards -1 as the reduction in fitness inflicted on the pre-evolutionary cells was greater than that observed in the post-evolutionary cells. This tendency was not observed in the absence of phenotypic constraints [Fig. 8(c)].

In this model, the phenotypic space is 100-dimensional, whereas the number of output genes is eight. Moreover, for genotypes evolved with $\tilde{P} = 1$, the interaction matrix \mathbf{O} between the gene regulatory network and the output gene is

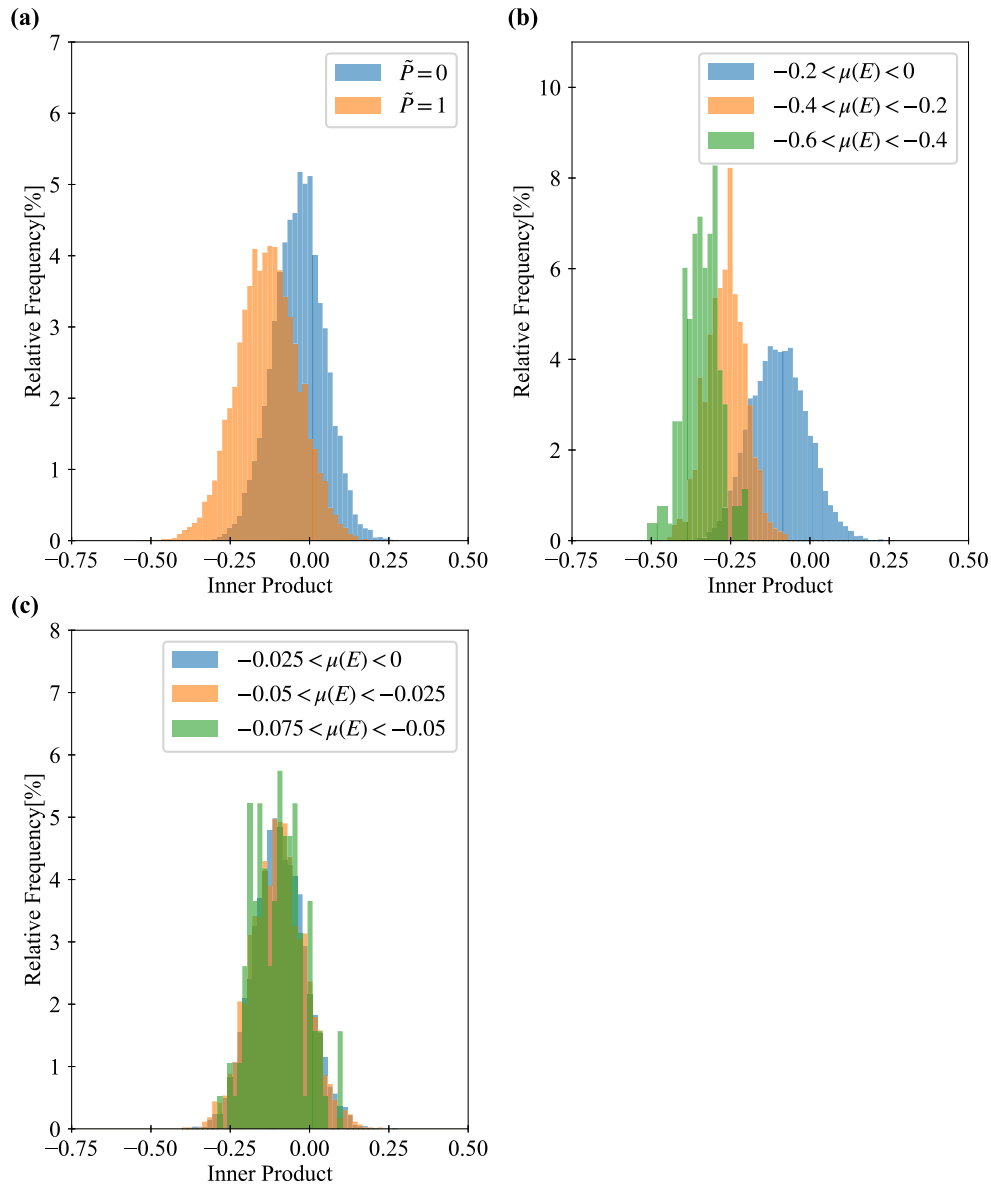


FIG. 8. (a) Histogram of cosine similarity $S_c(\mathbf{E}) = (\delta\mathbf{x}_{env}^*(\mathbf{E}) \cdot \delta\mathbf{x}_{evo}^*(\mathbf{E})) / \|\delta\mathbf{x}_{env}^*(\mathbf{E})\| \|\delta\mathbf{x}_{evo}^*(\mathbf{E})\|$. The blue histogram represents the data of the genotypes evolved under $\tilde{P} = 0$. The orange histogram represents the data for the genotypes that evolved under $\tilde{P} = 1$, and we can see that the distribution shifts more negatively when there is a one-dimensional phenotypic constraint. (c) Histograms of (a) are divided into several parts according to the degree of fitness. (b) When $\tilde{P} = 0$, the shape and position of the distribution do not change even if the fitness changes, but when $\tilde{P} = 1$, the larger the change in fitness, the more the distribution shifts in the negative direction.

effectively a rank 1 matrix as a result of the evolution, with each row vector approximately 80% correlated. This implies that a large number of phenotypic patterns capable of realizing a given target pattern exist. Accordingly, there is a huge variety of phenotypic changes that cancel out changes in fitness caused by environmental stress. When phenotypic constraints

are present, phenotypic changes due to adaptive evolution are more likely to occur along these constraints in the direction opposite to that of the response to environmental stress. In fact, in Fig. 8, the distribution of the cosine-similarity extends to the negative region in the presence of phenotypic constraints.

[1] Q. Zhang, G. Lambert, D. Liao, H. Kim, K. Robin, C.-k. Tung, N. Pourmand, and R. H. Austin, Acceleration of emergence of bacterial antibiotic resistance in connected microenvironments, *Science* **333**, 1764 (2011).

[2] R. R. Watkins and R. A. Bonomo, Overview: Global and local impact of antibiotic resistance, *Infect. Dis. Clin.* **30**, 313 (2016).

[3] P. Gilbert and A. J. McBain, Potential impact of increased use of biocides in consumer products on preva-

- lence of antibiotic resistance, *Clin. Microbiol. Rev.* **16**, 189 (2003).
- [4] S. B. Levy and B. Marshall, Antibacterial resistance worldwide: Causes, challenges and responses, *Nat. Med.* **10**, S122 (2004).
- [5] D. P. Gnanadhas, S. A. Marathe, and D. Chakravorty, Biocides-resistance, cross-resistance mechanisms and assessment, *Expert Opin. Invest. Drugs* **22**, 191 (2013).
- [6] V. Lázár, G. Pal Singh, R. Spohn, I. Nagy, B. Horváth, M. Hrtyan, R. Busa-Fekete, B. Bogos, O. Méhi, B. Csörgő *et al.*, Bacterial evolution of antibiotic hypersensitivity, *Mol. Syst. Biol.* **9**, 700 (2013).
- [7] L. Imamovic and M. O. Sommer, Use of collateral sensitivity networks to design drug cycling protocols that avoid resistance development, *Sci. Transl. Med.* **5**, 204ra132 (2013).
- [8] S. Suzuki, T. Horinouchi, and C. Furusawa, Prediction of antibiotic resistance by gene expression profiles, *Nat. Commun.* **5**, 5792 (2014).
- [9] M. O. Sommer, C. Munck, R. V. Toft-Kehler, and D. I. Andersson, Prediction of antibiotic resistance: Time for a new preclinical paradigm?, *Nat. Rev. Microbiol.* **15**, 689 (2017).
- [10] S. Suzuki, T. Horinouchi, and C. Furusawa, Acceleration and suppression of resistance development by antibiotic combinations, *BMC Genomics* **18**, 328 (2017).
- [11] M. Rodríguez de Evgrafov, H. Gumpert, C. Munck, T. T. Thomsen, and M. O. Sommer, Collateral resistance and sensitivity modulate evolution of high-level resistance to drug combination treatment in *Staphylococcus aureus*, *Mol. Biol. Evol.* **32**, 1175 (2015).
- [12] E. Toprak, A. Veres, J.-B. Michel, R. Chait, D. L. Hartl, and R. Kishony, Evolutionary paths to antibiotic resistance under dynamically sustained drug selection, *Nat. Genet.* **44**, 101 (2012).
- [13] A. J. Lopatkin, S. C. Bening, A. L. Manson, J. M. Stokes, M. A. Kohanski, A. H. Badran, A. M. Earl, N. J. Cheney, J. H. Yang, and J. J. Collins, Clinically relevant mutations in core metabolic genes confer antibiotic resistance, *Science* **371**, eaba0862 (2021).
- [14] Y. Taniguchi, P. J. Choi, G.-W. Li, H. Chen, M. Babu, J. Hearn, A. Emili, and X. S. Xie, Quantifying *E. coli* proteome and transcriptome with single-molecule sensitivity in single cells, *Science* **329**, 533 (2010).
- [15] M.-J. Han and S. Y. Lee, The *Escherichia coli* proteome: Past, present, and future prospects, *Microbiol. Mol. Biol. Rev.* **70**, 362 (2006).
- [16] J. Yuan, C. D. Doucette, W. U. Fowler, X.-J. Feng, M. Piazza, H. A. Rabitz, N. S. Wingreen, and J. D. Rabinowitz, Metabolomics-driven quantitative analysis of ammonia assimilation in *E. coli*, *Mol. Syst. Biol.* **5**, 302 (2009).
- [17] T. Horinouchi, S. Suzuki, H. Kotani, K. Tanabe, N. Sakata, H. Shimizu, and C. Furusawa, Prediction of cross-resistance and collateral sensitivity by gene expression profiles and genomic mutations, *Sci. Rep.* **7**, 14009 (2017).
- [18] T. Horinouchi, K. Tamaoka, C. Furusawa, N. Ono, S. Suzuki, T. Hirasawa, T. Yomo, and H. Shimizu, Transcriptome analysis of parallel-evolved *Escherichia coli* strains under ethanol stress, *BMC Genomics* **11**, 579 (2010).
- [19] S. M. Carroll and C. J. Marx, Evolution after introduction of a novel metabolic pathway consistently leads to restoration of wild-type physiology, *PLoS Genet.* **9**, e1003427 (2013).
- [20] L. Keren, O. Zackay, M. Lotan-Pompan, U. Barenholz, E. Dekel, V. Sasson, G. Aidelberg, A. Bren, D. Zeevi, A. Weinberger *et al.*, Promoters maintain their relative activity levels under different growth conditions, *Mol. Syst. Biol.* **9**, 701 (2013).
- [21] K. Kaneko, C. Furusawa, and T. Yomo, Universal relationship in gene-expression changes for cells in steady-growth state, *Phys. Rev. X* **5**, 011014 (2015).
- [22] T. Horinouchi, S. Suzuki, T. Hirasawa, N. Ono, T. Yomo, H. Shimizu, and C. Furusawa, Phenotypic convergence in bacterial adaptive evolution to ethanol stress, *BMC Evol. Biol.* **15**, 180 (2015).
- [23] E. Stolovicki and E. Braun, Collective dynamics of gene expression in cell populations, *PLoS ONE* **6**, e20530 (2011).
- [24] C. Furusawa and K. Kaneko, Global relationships in fluctuation and response in adaptive evolution, *J. R. Soc., Interface* **12**, 20150482 (2015).
- [25] C. Furusawa and K. Kaneko, Formation of dominant mode by evolution in biological systems, *Phys. Rev. E* **97**, 042410 (2018).
- [26] T. U. Sato and K. Kaneko, Evolutionary dimension reduction in phenotypic space, *Phys. Rev. Res.* **2**, 013197 (2020).
- [27] M. Tikhonov, S. Kachru, and D. S. Fisher, A model for the interplay between plastic tradeoffs and evolution in changing environments, *Proc. Natl. Acad. Sci. USA* **117**, 8934 (2020).
- [28] L. Glass and S. A. Kauffman, The logical analysis of continuous, non-linear biochemical control networks, *J. Theor. Biol.* **39**, 103 (1973).
- [29] E. Mjolsness, D. H. Sharp, and J. Reinitz, A connectionist model of development, *J. Theor. Biol.* **152**, 429 (1991).
- [30] I. Salazar-Ciudad, S. Newman, and R. Solé, Phenotypic and dynamical transitions in model genetic networks I. Emergence of patterns and genotype-phenotype relationships, *Evol. Dev.* **3**, 84 (2001).
- [31] K. Kaneko, Evolution of robustness to noise and mutation in gene expression dynamics, *PLoS ONE* **2**, e434 (2007).
- [32] M. Inoue and K. Kaneko, Entangled gene regulatory networks with cooperative expression endow robust adaptive responses to unforeseen environmental changes, *Phys. Rev. Res.* **3**, 033183 (2021).
- [33] S. Nagata and M. Kikuchi, Emergence of cooperative bistability and robustness of gene regulatory networks, *PLoS Comput. Biol.* **16**, e1007969 (2020).
- [34] We adopted this specified GRN model, whereas the following results on the dimension reduction and prediction of cross-resistance do not depend on this specific choice, as will be supported by the potential theory in Sec.V. We adopted a simplified model, to demonstrate that the evolved network showed a correlated response in antibiotics. For instance, we used threshold function $f(x)$, rather than Hill-function-based expression dynamics, for the simplicity of the evolution simulation. In previous studies, we adopted both these threshold function models and Hill-type functions [K. Fujimoto, S. Ishihara, and K. Kaneko, Network evolution of body plans, *PLoS ONE* **3**, e2772 (2008)]. We also adopted symmetric models [31] for the evolution of gene expression networks. As for the basic properties, concerning the nature of robustness in evolution and the correlation between environmental response and genetic response, the simplified model with threshold function with symmetry and models dropping these simplifications show

- the same result for numerical evolution. Hence, this paper is performed by a simplified and specific model.
- [35] W. H. Press and S. A. Teukolsky, Adaptive stepsize Runge-Kutta integration, *Comput. Phys.* **6**, 188 (1992).
- [36] A. Sakata and K. Kaneko, Dimensional reduction in evolving spin-glass model: Correlation of phenotypic responses to environmental and mutational changes, *Phys. Rev. Lett.* **124**, 218101 (2020).
- [37] In previous studies [25,36] using catalytic chemical reaction networks, one-dimensional phenotypic constraints correlated with growth rate were acquired even in evolution among multiple environments. In the present paper, a gene regulatory network model that does not include growth rate was used to consider higher dimensional phenotypic constraints.
- [38] See Supplemental Material at <http://link.aps.org/supplemental/10.1103/PhysRevResearch.5.043222> for detailed analysis and theoretical representation of phenotypic constraints and additional analysis of experimental data. It also includes Refs. [51,52].
- [39] Here we used cosine similarity as a measure of similarity of phenotypic change. A similar result can be obtained by using the correlation coefficient instead. Considering the correspondence with the results in Sec. 2, we consistently use the cosine similarity in the present paper.
- [40] Note that the existence of a genotype $\mathbf{G}^*(\mathbf{E})$ may not always be guaranteed. However, as the dimension of the genotypic space is much larger than that of the phenotypic space, such a genotype may exist. In Sec. IV, for any given environmental stress, the fitness in an environmental stress reaches maximal, through the adaptive evolution. Accordingly, $\mathbf{G}^*(\mathbf{E})$ exists at least in our model simulations.
- [41] The relative MIC $R_{MIC}(A^{(k)}, A^{(l)})$ is the quantity corresponding to the cross-fitness in this paper. Cross-resistance $r_{MIC}(A^{(k)}, A^{(l)})$ is represented as $r_{MIC}(A^{(k)}, A^{(l)}) = R_{MIC}(A^{(k)}, A^{(l)}) - R_{MIC}(ND, A^{(l)}) = MIC(A^{(k)}, A^{(l)}) - MIC(ND, A^{(l)})$, which is consistent with commonly used cross-resistance.
- [42] T. Tlustý, A. Libchaber, and J.-P. Eckmann, Physical model of the genotype-to-phenotype map of proteins, *Phys. Rev. X* **7**, 021037 (2017).
- [43] B. Xue, P. Sartori, and S. Leibler, Environment-to-phenotype mapping and adaptation strategies in varying environments, *Proc. Natl. Acad. Sci. USA* **116**, 13847 (2019).
- [44] V. Alba, J. E. Carthew, R. W. Carthew, and M. Mani, Global constraints within the developmental program of the *Drosophila* wing, *eLife* **10**, e66750 (2021).
- [45] Q.-Y. Tang, T. S. Hatakeyama, and K. Kaneko, Functional sensitivity and mutational robustness of proteins, *Phys. Rev. Res.* **2**, 033452 (2020).
- [46] K. Husain and A. Murugan, Physical constraints on epistasis, *Mol. Biol. Evol.* **37**, 2865 (2020).
- [47] J. S. Chuang, Z. Frentz, and S. Leibler, Homeorhesis and ecological succession quantified in synthetic microbial ecosystems, *Proc. Natl. Acad. Sci. USA* **116**, 14852 (2019).
- [48] A. Posfai, T. Taillefumier, and N. S. Wingreen, Metabolic trade-offs promote diversity in a model ecosystem, *Phys. Rev. Lett.* **118**, 028103 (2017).
- [49] E. Mori, C. Furusawa, S. Kajihata, T. Shirai, and H. Shimizu, Evaluating ^{13}C enrichment data of free amino acids for precise metabolic flux analysis, *Biotechnol. J.* **6**, 1377 (2011).
- [50] https://github.com/Takuya-U-Sato/Prediction_of_Cross-Fitness.
- [51] T. Tao, V. Vu, and M. Krishnapur, Random matrices: Universality of ESDs and the circular law, *Ann. Probab.* **38**, 2023 (2010).
- [52] T. Tao, Outliers in the spectrum of iid matrices with bounded rank perturbations, *Probab. Theory Relat. Fields* **155**, 231 (2013).